‘

Fungateria

Deliverable 4.2/v.1
A catalog of mapping between ELM topologies and patterns of their electrical activity

Project Number: 101071145

Project Acronym: FUNGATERIA

Project title: Enlisting synthetic fungal-bacteria consortia to produce multi-cellular mycelium-based ELMs with computational capability

Project start: 01 November 2022

Project duration: 48 months

European Innovation Council

Fungateria

DELIVERABLE FACTSHEET

Project Acronym | Number		FUNGATERIA | 101071145	
Deliverable Title:	A catalog of mapping between ELM topologies and patterns of their electrical activity		
Deliverable Description:	The tasks reported on here relate to the mapping of topologies of the engineered living materials (ELM) and correlated patterns of extracellular electrical activity. The report introduces the use of micro-electrode arrays (MEAs) for recording the electrical potentials of populations of bacteria and mycelium contained within co-cultures. MEAs have previously been used to catalog the extra-cellular potentials of neural tissue organoids and bacteria amongst other ELMs. Key findings are as follows. Electrical potential activity in the range of 10s-100 of µV (band-pass filtered at 0.0001 and 10 Hz) were consistently detected across channels. The amplitudes, spike widths and ISIs as well as the full extent of electrical potential activity support baseline comparisons with neural tissue, bacteria, etc. recorded using MEAs in the literature. Mono-cultures of bacteria are shown to have shorter extents of activity than co-cultures with Schizophyllum commune. Finally, differences in the correlation and mutual information for each of the co-cultures suggest further work is needed to assess morphological changes in-vitro during recordings particularly for the co-cultures of Bacillus subtilis. The effects of biofilm formation should also be investigated using similar techniques.		
Keywords:			
Due Date:	30-04-2024	**Date of submission:**	20-06-2025
Month of Project:	M18	**Version/Status:**	v2
Dissemination level:	PU – Public	**Dissemination type:**	R – Report
Report leader:	UWE	**Related WP task:**	WP4/T4.1
Editor(s):	UWE, KADK		
Partner Contributions:	UWE, UU, KADK		
Final review and approval:	KADK		

Document change history		
Date	**Authors**	**Description**
20.06.2025	UWE	Implementation of requested revisions providing greater specificity beyond general culture types, and describe how distinct physical or morphological features correlate with electrical activity.

The FUNGATERIA project has received funding from the European Union's HORIZON-EIC-2021-PATHFINDER CHALLENGES programme under grant agreement No. 101071145

Co-funded by the European Union

European Innovation Council

Fungateria

PROJECT CONSORTIUM

	Name	Short Name	Country
1.	DET KONGELIGE DANSKE KUNSTAKADEMIS SKOLER FOR ARKITEKTUR, DESIGN OG KONSERVERING	KADK	DK
2.	VRIJE UNIVERSITEIT BRUSSEL	VUB	BE
3.	UNIVERSITEIT GENT	UGent	BE
4.	UNIVERSITEIT UTRECHT	UU	NL
5.	UNIVERSITETET I OSLO	UIO	NO
6.	UNIVERSITY OF THE WEST OF ENGLAND, BRISTOL	UWE	UK
7.	DIMOKRITIO PANEPISTIMIO THRAKIS	DUTH	GR

TABLE OF CONTENTS

1 Background 4
2 ELM Topologies 5
3 Experimental Interface and Methods 6
4 Analysis of electrical activity 8
5 Conclusion 14
6 References 16

The FUNGATERIA project has received funding from the European Union's HORIZON-EIC-2021-PATHFINDER CHALLENGES programme under grant agreement No. 101071145

Co-funded by the European Union

European Innovation Council

1 Background

Organisms generate electromagnetic fields and employ the fields to obtain and fuse information about their environment, to establish communication between components of their bodies and to control the shape of their bodies [9, 10, 11, 13, 14, 16, 23, 24, 25, 38]. From an information processing point of view, one from the most interesting phenomena of bio-electricity is neural spiking. Spikes of electrical potential are the most well-known attributes of neurons and are attributed to their learning and decision making [5, 7, 33]. Not only neurons, but most living substrates can produce spikes of electrical potential. These include Protozoa [12, 17, 30], Hyrdoroza [19], slime moulds [20, 21] and plants [18, 36, 39].

Action potential-like spiking activity in fungi was first documented in 1976 [34], further confirmed in 1995 [29] and techniques for recording the electrical activity in fruiting bodies and colonised substrates was identified in 2018 [1]. While trying to uncover mechanisms of integrative electrical communication in fungi, we recorded and analysed electrical activity of oyster fungi *Pleurotus djamor* [1], bracket fungi *Ganoderma resinaceum* [3], ghost fungi (*Omphalotus nidiformis*), Enoki fungi (*Flammulina velutipes*), split gill fungi (*Schizophyllum commune*) and caterpillar fungi (*Cordyceps militaris*) [2]. We found significant degrees of variability of electrical spiking characteristics and substantial complexity of the electrical communication events [15].

Electrical activity of biofilms of bacteria was reported as early as 1964 in relation to electrical currents generated by microbial films of dental plaque [31]. Further studies demonstrated that ion channels conduct long-range electrical signals within bacterial biofilms via travelling waves of potassium [32]. Bacteria utilise electrical potentials in their homeostatic interactions with the local environment [26] and interaction across the bacterial colonies [32]. In single-cell form of <10 μm, bacteria can perceive stimuli from limited areas within constrained time-frames. Conversely, as members of larger assemblies, such as colonies or bio-films, individual bacteria sense and communicate with neighbouring cells, contributing to coordinated growth, task distribution, and response to environmental stimuli. This organised activity resembles a kind of multi-cellular information processing substrate exhibiting aneural patterns of extracellular electrical spiking. A rich spectrum of action potential like electrical activity have been recorded in bacterial colonies cultures on micro-electrode arrays [27] with indications that bacterial colonies might process information in a way similar to neural tissue [8]. Oscillations of membrane electrical potential of solitary planktonic *E. coli* cells have been demonstrated [22]. Despite these studies, much of this activity is not categorised, complicating establishment of comprehensive dictionaries of electrical potentials and comparisons between fungal and bacterial extracellular potentials.

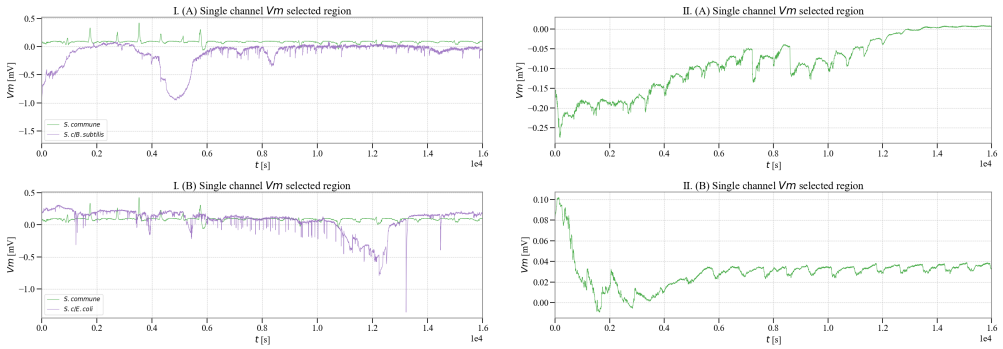

Figure 1: Zoomed to region of interest showing stereotypic extracellular electrical potentials (following band-pass filtering) f rom M EA r ecordings o f t he c o-cultures w ith m onocultures of mycelium I. (A) and (B) and contrast with monocultures of bacteria II. (A) and (B).

2 ELM topologies

In the context of Schizophyllum commune-based engineered living materials, ELM topologies refer to the physically and spatially organized architectures that emerge from the growth, structuring, and material integration of fungal mycelium within a given environment. These topologies go beyond simple culture types (e.g., agar plate, liquid suspension) to include specific, engineered geometries, dimensionalities, and boundary conditions of the living material. They are defined by features such as:

- Dimensionality (e.g., 2D surface mat vs. 3D scaffold colonization)
- Network density and branching architecture
- Substrate porosity and anisotropy
- Interface complexity (e.g., air–mycelium, mycelium–material, or mycelium–liquid bound-aries)
- Embedded scaffolds or patterns (e.g., microstructured lattices or channels)
- Constrained vs. open geometries (e.g., confined chambers, hydrogel moulds, porous membranes)

These topologies influence how the mycelium organizes itself into conductive and signalling networks, which in turn modulate how bioelectrical activity emerges, propagates, and is modulated across space and time. Distinct ELM topologies often give rise to characteristic spiking behaviours or electrophysiological signatures, due to their impact on biophysical properties such as ion transport, metabolic fluxes, and mechanical stress. Examples include:

- Dense, branched networks (e.g., in thick, compact ELMs) often exhibit low-amplitude, high-frequency spiking, potentially reflecting local metabolic or osmotic adjustments in tightly coupled hyphal masses.
- Sparse, exploratory hyphae at colony edges or within porous 3D scaffolds tend to show isolated high-amplitude spikes, possibly associated with sensing, foraging, or rapid environmental responses.

- Topologies with structured anisotropy (e.g., aligned fibers or microchannels) may exhibit directional propagation of electrical pulses, suggesting guidance of ionic flows along structural axes.
- Interfaces and boundary regions (e.g., air–substrate transitions) often show burst-like or oscillatory activity, potentially due to increased ion exchange, moisture variation, or light sensitivity.
- Topologically constrained geometries (e.g., microfluidic confinement or hydrogel wells) may enhance synchronization or feedback loops, resulting in patterned or rhythmic spike trains.

ELM topology fundamentally shapes the functional landscape of endogenous spiking.

3 Experimental interface and methods

Needle tipped macroscopic electrodes and microelectrode arrays (MEA) can be used for recording multi-cellular activity of bacterial and fungal cultures via extracellular electrical potentials. Invasive microelectrode or patch-clamp recordings are possible but not practical with mycelium and impossible with bacteria due to the size of the cells (corresponding to the size of a typical patch pipette) and the presence of a cell wall [27]. As such, this recording techniques is not suitable for recording of either individual bacteria or co-culture populations over mm length scales. Moreover, the object of our study is computing and sensing applications whereby dense arrays of recording electrodes numbering more than a single pair are preferred as is the use of populations rather than the isolated activity of the bioelectric fields of single microorganisms. MEAs provide a well characterised tool for investigation of the electrical potential activity of populations of bacteria and networks of hyphae. They have been used in experimental characterisation of the activity of excitable cells undergoing maturation, particularly neural tissue and populations of neurons [27]. For mono-cultures voltage sensitive dyes can be used. These approaches have seen success in optical recordings of bacteria [35]. However, the effects of such dyes are unknown for fungal-bacteria co-cultures. There are numerous difficulties with their implementation even in mono-cultures including poor signal to noise ratios, short recording durations and unknown long term impact on morphology, growth and electrical potential activity. Investigation of these effects and the possibility of use of genetically encoded voltage sensors could be useful in future but is currently outside of the scope of this study.

Fungal and bacterial culture The strain H4-8A of the split-gill fungus *Schizophyllum commune* was cultivated on *S. commune* minimal medium (SCMM) supplemented with 1.5% agar for a duration of three days at 30°C in a dark environment [28]. For co-cultures of fungi and bacteria the H4-8A strain cultivation methods were repeated with the addition of *E.coli* (strain: K-12 MG1655) and *B. subtilis* (strain: 168). Control plates containing only SCMM were also prepared. Sections of the samples were then transferred to a well plate with wells containing cellulose acetate membranes on top of SCMM. The cultures were cultivated in the well-plate a duration of three days at 30°C in a dark environment.

Preparation of fungal and bacterial cultures for MEA recordings: The contents of each well plate were removed and placed upside down into the recording chamber. The resulting structure comprised of the electrode recording surface contacting the layer of mycelium and/or bacteria growing on the cellulose acetate membrane. The SCMM medium contacted the cellulose acetate membrane but not the microelectrode array. The cultures contacted the full extent of the surface of the MEA including all single ended and reference electrodes. If there were gaps on the surface they could be seen through the clear acetate membrane and a replacement culture could be inserted. The cellulose membrane provided a physical separation between the SCMM below

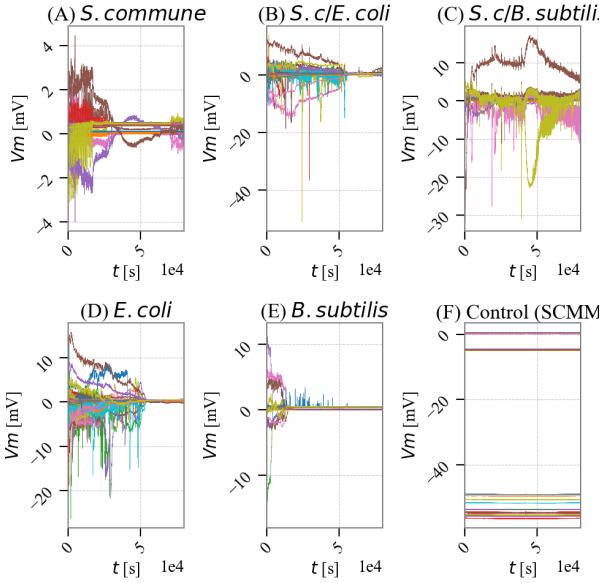

Figure 2: Raw data from micro-electrode array recordings of: (a) *Schizophyllum Commune*; (b) *Schizophyllum Commune* and *B.subtilis* for each of 59 channels (Ch1-59); (c) *Schizophyllum Commune* and *E.coli* for each of 59 channels (Ch1-59); (d) *E.coli* for each of 59 channels (Ch1-59) ; (e) *B.subtilis* for each of 59 channels (Ch1-59). The raw data is presented to provide an overview of the recording prior to filtering and analysis including comparison to the cellulose membrane/SCMM media control.

.

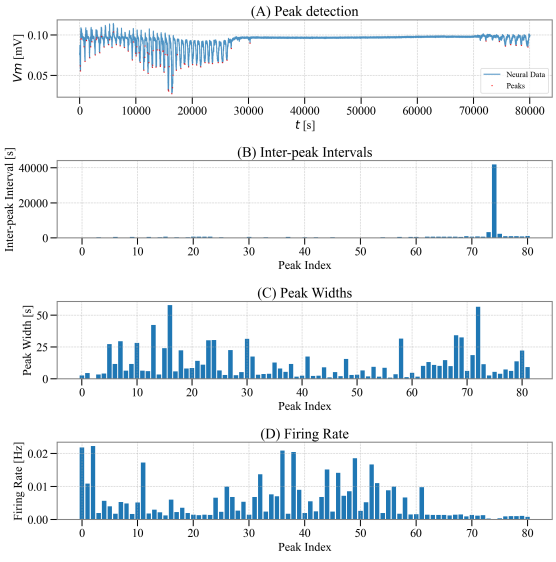

Figure 3: Single channel example of filtered data from *S. commune* monocultures showing the implemented approach to: (A) peak detection,(B) ISI estimation, (C) peak widths estimation, (D) firing rate.

and the mycelium. This allowed for the isolation of the mycelium and its extracellular electrical potentials from possible potentials induced by the ionic composition of the nutrient media. The cellulose membrane acted as a scaffold for the attachment of the bacteria and reduced the vertical surface area between the bacteria and the micro-electrodes. The isolation of signals from the bulk media was also apparent due to the low electrical conductivity of the cellulose membrane. This effect may explain the presence of extracellular potentials in the bacteria-containing samples without the formation of a biofilm. As a result the majority of bacterial cells were planktonic but attached to the membrane for both monocultures of bacteria and co-cultures with mycelium.

Micro-electrode arrays (MEAs) 60 channel hard gold plated MEAs (Multi-channel Systems, DE) were used for all recordings. The multi-channel signals were then recorded using a custom interface combined with sigma-delta based analog-to-digital converter dataloggers (Pico Technologies, UK). This resulted in data from 59 single ended electrode channels plus a reference electrode. The single ended electrodes in the MEA are arranged in a rectangular grid array with each electrode having a diameter of 100 μm and a spacing of 700 μm. MEAs were chosen for this study because bacteria are difficult to study using conventional intracellular methods such as patch clamp. This common method is ineffectual and cannot form a seal on the surface of the bacteria. Additionally there is no known method for successfully piercing the membrane of the bacteria without rendering the electrically inactive or indistinguishable from the volume media. MEAs have been used successfully in neural recordings and in development of organoid computing devices. MEAs record the sum of potentials originating from agglomerations of bacteria and/or mycelial hyphae as they are conducted by the proximate volume of the external media. Therefore recordings using this technique and the specific device resolve the activities of populations of hyphae and hyphal-bacterial matrices via local field potentials respectively. Initial filtering and analysis of recordings confirmed that magnitudes of potentials (10-100 μV) were similar compared with previous recordings using comparable techniques for mono-cultures of bacteria [27]. To the best of our knowledge, MEA recordings of fungal cultures and co-cultures are not available for comparison. MEA recordings of the action potentials of neural tissue have similar amplitudes being close to 1000 times lower amplitudes (e.g. 50 mV) than intracellular recordings when recorded in the same cellular region concurrently [6].

Filtering and data processing A band-pass filter range of 0.0001 hz and 10 hz was implemented to isolate biologically relevant activity. These ranges were based on previous firing rates for bacterial [27] and fungal [4] cultures respectively. A peak detection algorithm was implement in Python using the Scipy library [37]. For statistical analysis all channels were normalised taking absolute intensity values removing the effects of voltage biases.

4 Analysis of electrical activity

The electrical potentials analysis procedures are outlined for a single channel of the mycelium monoculture recordings in Fig. 3. Zoomed in regions of interest for mycelium monocultures and co-cultures are depicted in Fig. 1:I (A-B). Bacterial monocultures and related extracellular potentials are shown in regions of interest for a single channel in Fig. 1:II (A-B). The raw data for all 59 channels and before implementation of the band-pass filter is shown in Fig. 2. A live/dead assay was conducted using the *S.commune* cultures leading to a reduction and cessation of electrical potentials following application of the 5ml of 1.42M K+ dose at a t [s] of 1^2 secs. The high concentration of extracellular potassium impedes fungal electrical potential activity by depolarising the membrane potential and further causing depolarisation block or conduction block as shown in n Fig. 14. Controls conducted with cellulose membrane and nutrient media without mycelium showed an absence of electrical potentials as depicted Fig. 2:(F).

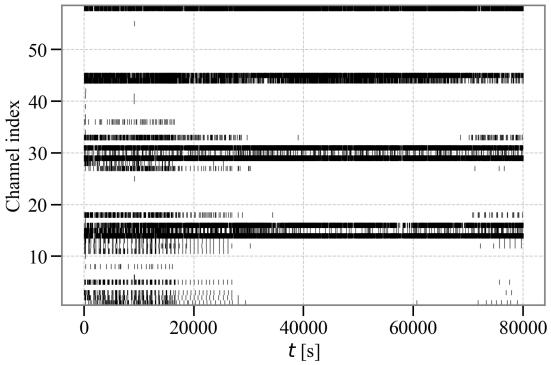

Figure 4: *S. commune* monoculture raster plot.

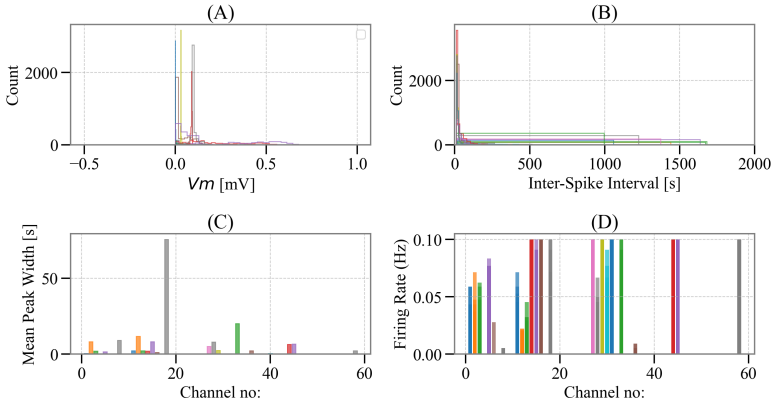

Figure 5: *S. commune* monoculture: (A) amplitudes of peaks, (B) inter-spike intervals, (C) mean peak widths per channel and (D) mean firing rate per channel.

Both mono-and-co-cultures displayed electrical spiking activity across multiple channels of the array. The resulting raster plot for channels 1-59 of the monocultures of *S. commune* are shown in Fig. 4 with analysis of amplitudes of peaks, inter-spike intervals (ISI), mean peak widths per channel and mean firing rate per channel listed in Fig. 5. The mean multi-channel combined amplitude of electrical potentials for the mycelium monocultures was Vm 0.07 [mV] (median = 0.04, σ= 0.1). A maximum amplitude Vm of 0.96 [mV] was also detected with some large amplitude signals evident within the band-pass filtered region. The widths of peaks had a mean t of 3.6 [s] (median = 1.4 [s], σ= 121.2 [s]). The mean t for ISI was 54.7 [s] (median = 17 [s], σ= 736.5 [s]). Large intervals were apparent as a result of waves of co-ordinated activity that then ceased for longer periods of time during the recording. For instance, a maximum t ISI for a single channel of 49,955 [s] was detected indicating long periods of cessation of extracellular potentials. Cessation was evident at c. 1e3 [s] with activity recommencing on some channels at 1e7 [s]. However, a significant number of channels show no cessation of activity for this time period. For the mycelial cultures, the mean firing rate was 0.056 Hz (median= 0.058 Hz, σ= 0.02 Hz).

Raster plots for both bacterial monocultures are shown in Fig. 6 and Fig. 8 respectively. The

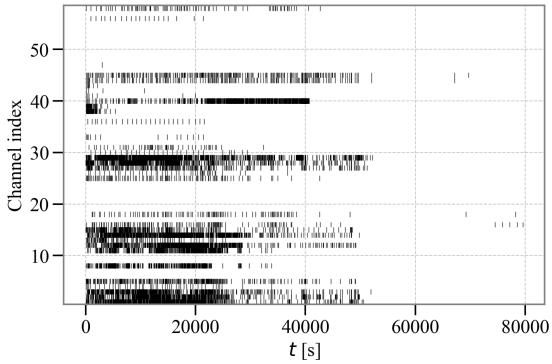

Figure 6: *E. coli* monoculture raster plot

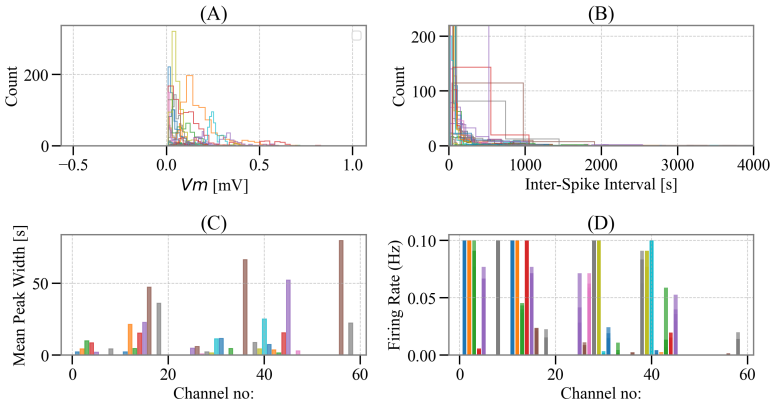

Figure 7: *E. coli*: (A) amplitudes of peaks, (B) inter-spike intervals, (C) mean peak widths per channel and (D) mean firing rate per channel.

analysis of the characteristics of electrical potentials for both monocultures are outlined in Fig. 7 and Fig. 9. The monocultures of bacteria showed the lowest extent of activity with cessation of electrical potentials identified as peaks at c. 1e5 [s] for *E. coli* and c. 1e2 for *B. subtilis*. A single channel (no. 40) in *B. subtilis* showed a much larger extent of activity until c. 1e6 [s]. The mean multi-channel amplitude Vm of peaks for *E. coli* was 0.07 [mV] (median = 0.04, σ= 0.09) and peak widths exhibited an average of 6.6 [s] (median = 1.6, σ= 28.9 [s]). The ISI for *E. coli* monocultures was 167.6 [s] (median = 53 [s], σ= 724.42 [s]). The firing rate mean was lower than monocultures of mycelium at 0.02 Hz (median = 0.018 Hz, σ= 0.02 Hz). The *B. subtilis* monocultures exhibited a multi-channel mean amplitude Vm of 0.22 [mV] (median = 0.14 [mV], σ= 0.2 [mV]). The mean peak width was 14 [s] (median= 0.55 [s], σ= 62 [s]). ISI results showed an average interval of 177 [s] (median= 53 [s], σ= 1422 [s]) and firing rates exhibted a mean rate of 0.02 Hz (median = 0.01 Hz, σ= 0.02 Hz).

Co-cultures raster plots show a longer extent of activity compared with both monocultures of bacteria and of mycelium as depicted in Fig. 12 for *E. coli* and Fig. **??** for *B. subtilis*. For *E. coli* co-cultures the extent of the activity was c. 1e6 [s] with a minority of channels (22 %) exhibiting electrical potentials until 1e8 [s]. The multi-channel combined mean amplitude for co-cultures of

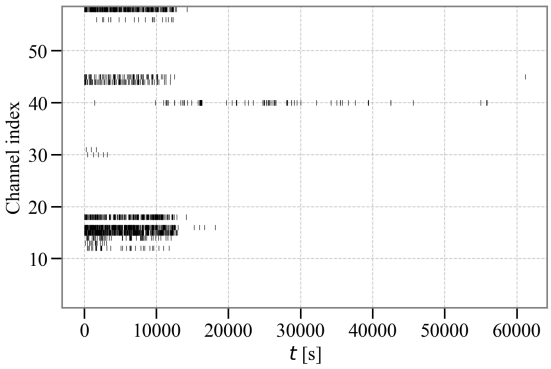

Figure 8: *B. subtilis* monoculture raster plot

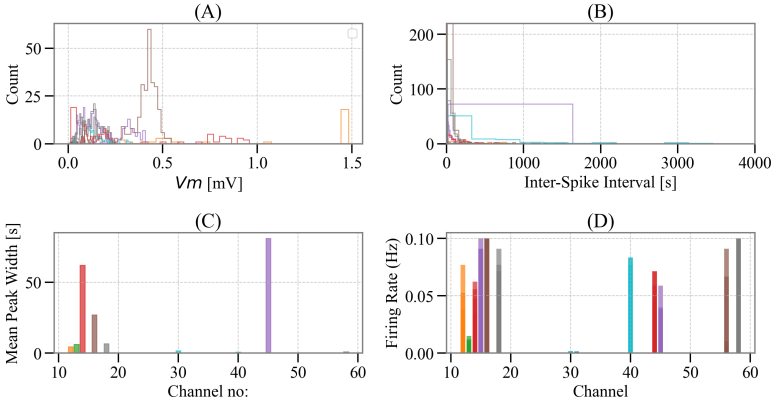

Figure 9: *B. subtilis* monoculture: (A) amplitudes of peaks, (B) inter-spike intervals, (C) mean peak widths per channel and (D) mean firing rate per channel.

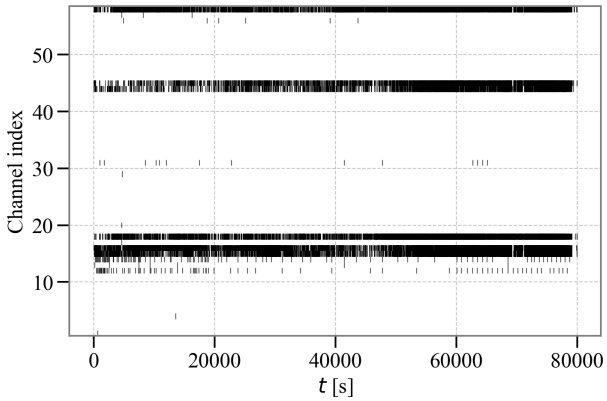

Figure 10: *B. subtilis* co-culture raster plots.

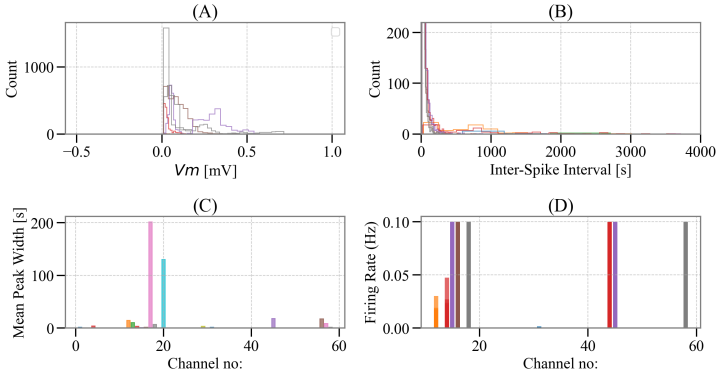

Figure 11: *B. subtilis* co-culture: (A) amplitudes of peaks, (B) inter-spike intervals, (C) mean peak widths per channel and (D) mean firing rate per channel

E. coli was Vm of 0.03 [mV] (median = 0.02 [mV], σ= 0.03 [mV]). Peak widths had a mean of 1.6 [s] (median= 0.39 [s], σ= 6.2 [s]). The ISI was detected to be 164.5 [s] (median= 47 [s], σ= 806 [s]). The co-cultures of *E. coli* showed a lower mean firing rate compared to the mean rate for monocultures of mycelium and bacteria at 0.029 Hz (median=0.02 Hz, σ=0.02). Co-cultures of *B. subtilis* exhbited mean amplitudes of peaks Vm of 0.08 [mV] (median = 0.03 [mV], σ= 0.12 [mV]). Peak widths averaged at 3.1 [s] across channels (median= 0.88 [s], σ= 12 [s]). The multi-electrode mean ISI was 57.1 [s] (median= 22 [s], σ= 444.5 [s]). Co-cultures of *B. subtilis* showed comparatively higher mean firing rates compared with *E. coli* co-cultures at 0.048 Hz (median=0.045 Hz, σ=0.026 Hz). Channel activity was less widely distributed in co-cultures of *B. subtilis* with a large number of channels showed reduced activity potentially related to deleterious effects of co-cultivation of this bacteria and *S. commune* mycelium.

The mutual information and correlation between the amplitudes of the electrical potentials was then analysed. The random electrical activity of the inoculated cultures becomes synchronised with an increasing degree of correlation as the network develops and this co-ordination of activity can be interpreted as morphological changes in the cultures. The extracellular potential dynamics of these developing biological networks enables the characterisation of this spatio-

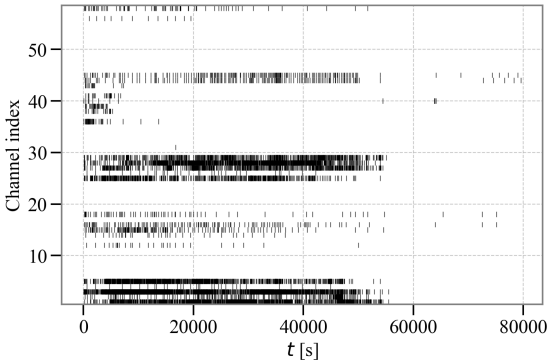

Figure 12: *E. coli* co-culture raster plot

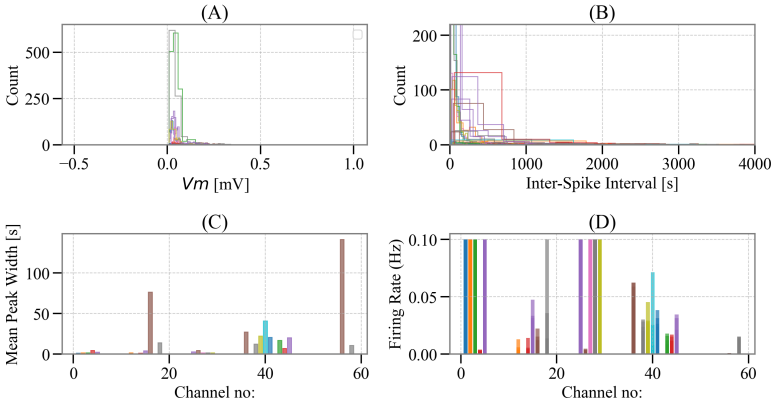

Figure 13: *E. coli* co-culture: (A) amplitudes of peaks, (B) inter-spike intervals, (C) mean peak widths per channel and (D) mean firing rate per channel

temporal organisation. The observed patterns of extracellular potentials provide evidence of cell –cell communication mechanisms in fungal-bacterial communities as evidenced in Fig. **??** where mean correlation values for *B. subtilis* co-cultures are higher than for monocultures. This suggests that, in terms of Vm magnitudes, the overall functional connectivity of the *B. subtilis* co-cultures is higher. Alternatively, this could be as a result of bacterial reduction in the region of the electrodes where extracellular electrical potentials from one cultured organism begin to dominate, hence the increased correlation. However, these results are not conclusive and more detailed investigation of the electrode region and temporal progression of correlation of different electrophysiological states is required. Mutual information in *E. coli* co-cultures showed relatively higher mean values than the monocultures of *S. commune* and the co-cultures with *B. subtilis*. Similarities with the mutual information values between *E. coli* co-cultures and the bacterial monocultures suggests a larger influence from this bacteria's electrical communications over a larger surface area in the cultures. The same similarities were not apparent in the co-cultures of *B. subtilis*.

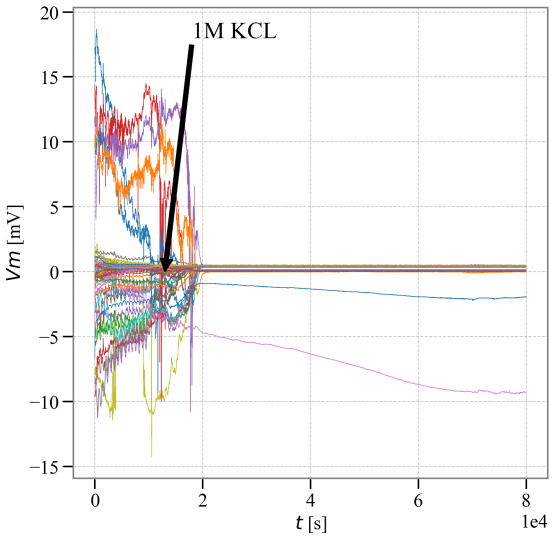

Figure 14: Cessation assay using application of a 1.42M K+ dose at a t of 1e1 [s] in the extracellular medium of *S.commune* (chamber size: 10mm ^{3}). This test validates the presence of live organisms in the MEA recordings due to the resulting cessation of extracellular electrical potential activity with a small delay related to diffusion. This graph shows the raw extracellular data from the MEA prior to band-pass filtering. Conduction block occurs as a result of accumulation of potassium leading to cessation of electrical activity.

5 Conclusion

Electrical potential activity in the range of 10s-100 of μV (band-pass filtered at 0.0001 and 10 Hz) were consistently detected across channels. The amplitudes, spike widths and ISIs as well as the full extent of electrical potential activity support baseline comparisons with neural tissue, bacteria, etc recorded using MEAs in the literature. The extent of activity is lengthened by co-culturing mycelium and bacteria for both species combinations compared with bacterial monocultures. Per-channel activity (i.e. number of active channels over time) is higher in co-cultures compared with monocultures of bacteria. Conduction block assays using potassium chloride can test cessation of ELM activity and presence of viable ELMs. Electrical potential magnitudes (Vm) post-filtering remain constant across monocultures and co-cultures providing evidence for the establishment of a catalog of stereotypic extracellular electrical potentials. Finally, differences in the correlation and mutual information for each of the co-cultures suggest further work is needed to assess morphological changes in-vitro during recordings particularly for the co-cultures of *B. subtilis*. The effects of biofilm formation should also be investigated using similar techniques.

MEA based recordings are a useful tool to study the spatiotemporal maturation and extracellular electrical potentials of colonies of bacteria and fungus. Here, the observed patterns of extracellular potentials provide evidence of cell–cell communication mechanisms in fungal-bacterial communities of different types dependent on the exact composition of the ELM. Further work could investigate the differences between planktonic and biofilm forming bacteria and entrainment of signals between bacterial and fungal consortia. ELM morphology and constituent bacteria and fungus have a clear impact on the resulting multi-cellular electrical potentials as

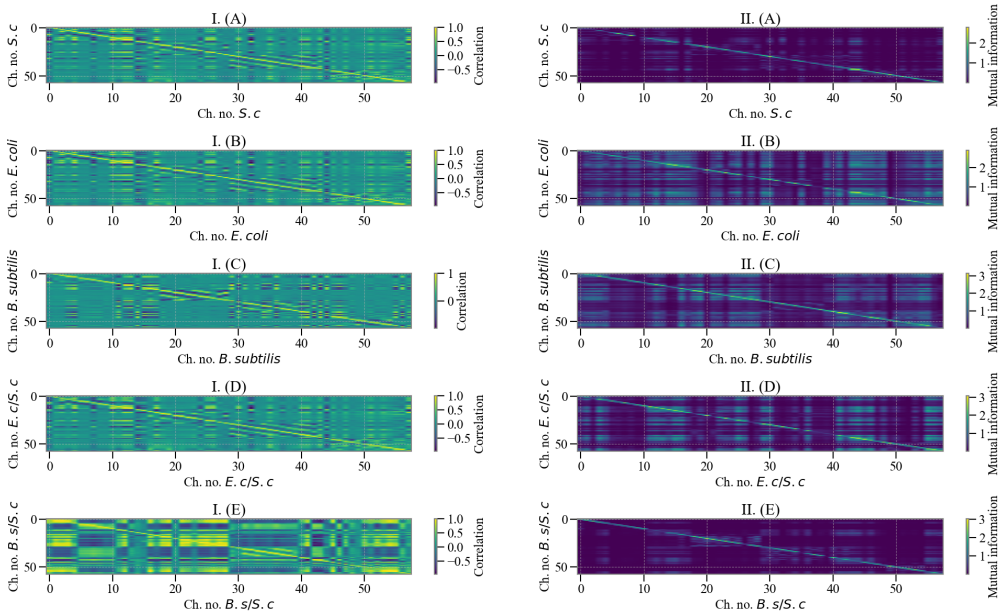

Figure 15: Per-channel correlation: I. (A) monocultures of mycelium,I. (B) monocultures of *E. coli*,I. (C) monocultures of *B. subtilis*;(E) co-cultures with *E. coli*. Mutual information: II. (A) monocultures of mycelium,II. (B) monocultures of *E. coli*,II. (C) monocultures of *B. subtilis*;II. (E) co-cultures with *E. coli*.

recorded via proximate micro-electrode arrays. This approach is likely to be suitable for the development of organoid computing platforms with scalable functionality not possible using conventional biological electrophysiology recording methods.

References

[1] Andrew Adamatzky. On spiking behaviour of oyster fungi Pleurotus djamor. *Scientific reports*, 8(1):1–7, 2018.

[2] Andrew Adamatzky. Language of fungi derived from their electrical spiking activity. *Royal Society Open Science*, 9(4):211926, 2022.

[3] Andrew Adamatzky and Antoni Gandia. On electrical spiking of ganoderma resinaceum. *Biophysical Reviews and Letters*, 0(0):1–9, 0.

[4] Andrew Adamatzky and Antoni Gandia. On electrical spiking of ganoderma resinaceum. *Biophysical Reviews and Letters*, 16(04):133–141, 2021.

[5] Daniela Sabrina Andres. The language of neurons: theory and applications of a quantitative analysis of the neural code. *International Journal of Medical and Biological Frontiers*, 21(2):133, 2015.

[6] Gary Banker and Kimberly Goslin. *Culturing nerve cells*. MIT press, 1998.

[7] Morris H Baslow. The languages of neurons: an analysis of coding mechanisms by which neurons communicate, learn and store information. *Entropy*, 11(4):782–797, 2009.

[8] Eshel Ben-Jacob. Learning from bacteria about natural information processing. *Annals of the New York Academy of Sciences*, 1178(1):78–90, 2009.

[9] R Beutner. Source of bioelectricity, investigated by the relation between stainability and electric charges in tissues and artificial models. *Proceedings of the Society for Experimental Biology and Medicine*, 27(1):44–46, 1929.

[10] R Beutner and J Lozner. The relation of life to electricity: Part viii the mechanism of oxidation-reduction potentials in living tissues. *Protoplasma*, 19:370–380, 1933.

[11] R Beutner and Joseph Lozner. The relation of life to electricity: Part iii stainability and electromotive forces of protein; the influence of watersoluble acids. *Protoplasma*, 12:145–160, 1931.

[12] MS Bingley. Membrane potentials in amoeba proteus. *Journal of Experimental Biology*, 45(2):251–267, 1966.

[13] HS Burr. Bioelectricity: potential gradients. *Medical physics*, 2:90–94, 1950.

[14] Kenneth S Cole and Howard J Curtis. Bioelectricity: electric physiology. *Medical physics*, 2:82–90, 1950.

[15] Mohammad Mahdi Dehshibi and Andrew Adamatzky. Electrical activity of fungi: Spikes detection and complexity analysis. *Biosystems*, 203:104373, 2021.

[16] WA Dorfman. Electrical polarity of the amphibian egg and its reversal through fertilization. *Protoplasma*, 21:245–257, 1934.

[17] R Eckert, Y Naitoh, and K Friedman. Sensory mechanisms in paramecium. i. *J. exp. Biol*, 56:683–694, 1972.

[18] Jörg Fromm and Silke Lautner. Electrical signals and their physiological significance in plants. *Plant, cell & environment*, 30(3):249–257, 2007.

[19] Alison Hanson. Spontaneous electrical low-frequency oscillations: a possible role in hydra and all living systems. *Philosophical Transactions of the Royal Society B*, 376(1820):20190763, 2021.

[20] Tatsuichi Iwamura. Correlations between protoplasmic streaming and bioelectric potential of a slime mold, *Physarum polycephalum*. *Shokubutsugaku Zasshi*, 62(735-736):126–131, 1949.

[21] Noburo Kamiya and Shigemi Abe. Bioelectric phenomena in the myxomycete plasmodium and their relation to protoplasmic flow. *Journal of Colloid Science*, 5(2):149–163, 1950.

[22] Joel M Kralj, Daniel R Hochbaum, Adam D Douglass, and Adam E Cohen. Electrical spiking in escherichia coli probed with a fluorescent voltage-indicating protein. *Science*, 333(6040):345–348, 2011.

[23] Michael Levin. Bioelectric mechanisms in regeneration: unique aspects and future perspectives. In *Seminars in cell & developmental biology*, volume 20, pages 543–556. Elsevier, 2009.

[24] Michael Levin. Bioelectric signaling: Reprogrammable circuits underlying embryogenesis, regeneration, and cancer. *Cell*, 184(8):1971–1989, 2021.

[25] Michael Levin and Christopher J Martyniuk. The bioelectric code: An ancient computational medium for dynamic control of growth and form. *Biosystems*, 164:76–93, 2018.

[26] Genaro J Martínez, Andrew Adamatzky, Kenichi Morita, and Maurice Margenstern. Computation with competing patterns in life-like automaton. In *Game of Life Cellular Automata*, pages 547–572. Springer, 2010.

[27] Elisa Masi, Marzena Ciszak, Luisa Santopolo, Arcangela Frascella, Luciana Giovannetti, Emmanuela Marchi, Carlo Viti, and Stefano Mancuso. Electrical spiking in bacterial biofilms. *Journal of The Royal Society Interface*, 12(102):20141036, 2015.

[28] Robin A Ohm, Jan F de Jong, Charissa de Bekker, Han AB Wösten, and Luis G Lugones. Transcription factor genes of schizophyllum commune involved in regulation of mushroom formation. *Molecular microbiology*, 81(6):1433–1445, 2011.

[29] S Olsson and BS Hansson. Action potential-like activity found in fungal mycelia is sensitive to stimulation. *Naturwissenschaften*, 82(1):30–31, 1995.

[30] Shunsuke Ooyama and Tatsuo Shibata. Hierarchical organization of noise generates spontaneous signal in paramecium cell. *Journal of theoretical biology*, 283(1):1–9, 2011.

[31] RB Parker and ML Snyder. Electrical potentials of the dental plaque. *Life Sciences*, 3(11):1275–1279, 1964.

[32] Arthur Prindle, Jintao Liu, Munehiro Asally, San Ly, Jordi Garcia-Ojalvo, and Gürol M Süel. Ion channels enable electrical communication in bacterial communities. *nature*, 527(7576):59–63, 2015.

[33] J Andrew Pruszynski and Joel Zylberberg. The language of the brain: real-world neural population codes. *Current opinion in neurobiology*, 58:30–36, 2019.

[34] Clifford L Slayman, W Scott Long, and Dietrich Gradmann. "action potentials" in neurospora crassa, a mycelial fungus. *Biochimica et Biophysica Acta (BBA)-Biomembranes*, 426(4):732–744, 1976.

[35] Hiroaki Suzuki, Zheng-Yu Wang, Mie Yamakoshi, Masayuki Kobayashi, and Tsunenori Nozawa. Probing the transmembrane potential of bacterial cells by voltage-sensitive dyes. *Analytical sciences*, 19(9):1239–1242, 2003.

[36] Kazimierz Trebacz, Halina Dziubinska, and Elzbieta Krol. Electrical signals in long-distance communication in plants. In *Communication in plants*, pages 277–290. Springer, 2006.

[37] Pauli Virtanen, Ralf Gommers, Travis E Oliphant, Matt Haberland, Tyler Reddy, David Cournapeau, Evgeni Burovski, Pearu Peterson, Warren Weckesser, Jonathan Bright, et al. Scipy 1.0: fundamental algorithms for scientific computing in python. *Nature methods*, 17(3):261–272, 2020.

[38] Jessica L Whited and Michael Levin. Bioelectrical controls of morphogenesis: from ancient mechanisms of cell coordination to biomedical opportunities. *Current opinion in genetics & development*, 57:61–69, 2019.

[39] Matthias R Zimmermann and Axel Mithöfer. Electrical long-distance signaling in plants. In *Long-Distance Systemic Signaling and Communication in Plants*, pages 291–308. Springer, 2013.